

Original Research Article

Active and Time delay Controls on Dynamical of The Micro-Electro-Mechanical System (MEMS) Resonator

Comment [WU1]: What is dynamical please explain, I do not agree with the title of the article.

Abstract

In this paper, the active control and time delay control are applied on a nonlinear dynamic mechanical system subjected to external force to reduce the resulted vibration. The system is modeled by a unique nonlinear differential equation. We applied the technique of multiple scale perturbation to obtain an approximate solution and showing the response equation. The primary resonance case is investigated to study the stability and the steady-state response of the system. Also we studied the linearity of the solution. MATLAB 14.0 and Maple 18.0 programs were used to study the numerical solution and the effect of the different parameters for the response of the nonlinear dynamic mechanical system.

Comment [WU2]: In title you mention "Dynamical controls, whereas in abstract you are talking about nonlinear dynamic" justify

Comment [WU3]: Re-write

Keywords

Nonlinear dynamical system, Active Control, time delay, multiple scale perturbation method.

1. Introduction

In recent years, several investigations have reported how to control the vibration of dynamical systems. The dynamic absorber is one of the most common methods of vibration control that it has low cost, simple operation and taking advantage of the saturation phenomenon. This phenomenon has been observed in the forced vibrations of coupled two degrees of freedom systems with quadratic nonlinearities in the presence of both internal and primary resonances. Vazquez-Gonzalez and Silva Navarro [1] discussed the dynamic response and nonlinear frequency analysis of a damped Duffing system attached to an autoparametric pendulum absorber, operating under the external and internal resonance conditions. They deduced that is possible to reduce simultaneously the amplitude responses of the primary and secondary systems for excitation frequencies close to the exact tuning.

Comment [WU4]: This long introduction does not attract the reader and can't see any interested research orientated statement. Please re-do the intro section. Also the overall English of the paper is poor.

Eissa et al. [2] reported the results of studying the vibration reduction of a nonlinear spring pendulum subjected to multi external and parametric excitations. They investigated that the vibration of a ship pitch-roll motion can be reduced using a longitudinal absorber. Active absorber for non-linear vibrating system subjected to external and parametric forces is investigated by Sayed and Kamel [3]. Sado [4] described the numerical simulation of a nonlinear two-mass auto parametric system with elastic pendulum hangs down from the flexible suspended body. He showed that near the internal and external resonances depending on a selection of physical system parameters, the amplitudes of vibrations of coupled modes may be differently.

Wenzhi and Zhiyong [5] studied active control of torsional vibration of a large turbo-generator. They found that full state feedback control with linear quadratic regulator (LQR) has significant effectiveness on attenuation of torsional vibration energy and response of the turbo-generator's shaft system.

45 Amer et al. [6] used two active control laws based on the linear negative velocity and
46 acceleration feedback and showed that the acceleration feedback was good for the main system.
47 Hegazy and Salem [7] presented the numerical and perturbation solutions of an inclined beam to
48 external and parametric forces with two different controllers, positive position feedback (PPF)
49 and nonlinear saturation controllers (NSC) and found that the (NSC) one is an effective
50 controller.

51 El-Gohary and El-Ganaini [8] studied applying a time delay absorber to suppress chaotic
52 vibrations of a beam under multi-parametric excitations. They concluded that the vibration of the
53 main system can be reduced. They showed that time-delay effect on the frequency response
54 curves is trivial. Maccari [9] investigated the periodic solutions for parametrically excited system
55 under state feedback control with a time delay. He has derived two slow-flow equations,
56 governing the amplitude and phase of approximate long time response. Elnaggar and Khalil [10]
57 investigated the response of nonlinear system subjected to external excitation controlled by the
58 appropriate choice of feedback gains and two distinct time delays. They found that a suitable
59 choice of the feedback gains and time-delays can enlarge the critical force amplitude, and reduce
60 the peak amplitude of the response (or peak amplitude of the free oscillation term) for the case of
61 primary resonance or for the case of super harmonic resonance. El-Bassiouny and El-Kholy [11]
62 discussed the resonances of a nonlinear single-degree-of-freedom system with time delay in
63 linear feedback control. They observed from the frequency-response curves of primary resonance
64 that the response amplitude loses stability for increasing time delay.

65 A study for (NSC) is presented by Hamed and Amer [12] that used to suppress the vibration
66 amplitude of a structural dynamic model simulating nonlinear composite beam at simultaneous
67 sub-harmonic and internal resonance excitation. Kamel et al. [13] studied the active vibration
68 control of a nonlinear magnetic levitation system via (NSC). Warminski et al. [14] presented an
69 application of (NSC) algorithm for a self-excited strongly nonlinear beam structure driven by an
70 external force. The results show that the increase in controller damping may cancel the
71 undesirable instability. Amer [15] investigated the behavior of the coupling of two non-linear
72 oscillators of the system and absorber representing ultrasonic cutting process subjected to
73 parametric excitation. He showed that the steady state amplitude of the main system is a
74 monotonic increasing function of the excitation force amplitude up to a saturation value. The
75 multiple scales method was used by Ebrahimi et al [16] to perform a nonlinear vibrational
76 analysis of a sliding pendulum in two cases with dry and lubricated clearance joint. They
77 investigated that in the primary resonance analysis, increasing the dynamic lubricant viscosity
78 decreases the amplitude in the vicinity of the linear natural frequency as expected.

79 Amer and Abd Elsalam [17] studied the stability of a nonlinear two-degree of freedom system
80 subjected to multi excitation forces at simultaneous primary and internal resonance case. They
81 deduced that the steady state amplitude is monotonic increasing function of the excitation force
82 amplitude increased and is a monotonic decreasing of the damping coefficient. The study of
83 forced nonlinear vibrations of a simply supported Euler-Bernoulli beam resting on a nonlinear
84 elastic foundation with quadratic and cubic nonlinearities with the homotopy analysis method
85 has presented by Shahlai-Far et al. [18]. The derived closed-form solution of the amplitude
86 yields frequency response curves for various values of the quadratic and cubic nonlinearity
87 coefficients presenting their softening/hardening-type effect on the distributed-parameter system.

88 Many applications of controlling the dynamical systems which investigated in more papers.
89 Wang et al. [19] investigated the dynamic response and bifurcation characteristics of blades with
90 varying rotating speed. The results of the paper showed the interaction of the fluid and the

91 structure that the opposite varying trends for the amplitudes and phase angles with respect to the
 92 system parameters indicate the energy transfer between the vibrations of the fluid and the
 93 structure. Hamed et al. [20] were investigated the nonlinear vibrations and stability of the MEMS
 94 gyroscope subjected to different types of parametric excitations. They applied an active vibration
 95 controller to reduce the resulted vibration. A multi-modal flexible wind turbine model with
 96 variable rotor speed has been formulated by Staino and Basu [21] using a Lagrangian approach.
 97 They analyzed the effect of the rotational speed on the edgewise vibration of the blades. They
 98 deduced according to the numerical results which have been presented in their paper, a
 99 considerable deterioration of the structural response of the blade could occur caused by
 100 variations in the rotational speed due to an electrical fault.

101 Shao et al. [22] studied the effect of time-delayed feedback controller on the dynamics of
 102 electrostatic MEMS resonators. They compared the results of the perturbation method to the
 103 shooting technique and the basin-of-attraction analysis. They found that the shooting technique
 104 performs well in predicting the global stability for the resonator under negative gain control. In a
 105 MEMS system, Daqaq et al. [23] again used the method of multiple of scales to define a first-
 106 order nonlinear approximate solution, which was then employed to redefine the impulse
 107 sequence of a ZV input shaper to minimize residual oscillation in a torsional micromirror. Static
 108 and Dynamic Mechanical Behaviors of Electrostatic MEMS Resonator with Surface Processing
 109 Error is studied by Feng et al [24]. They showed the resonance frequency and bifurcation
 110 behavior through dynamic analysis.

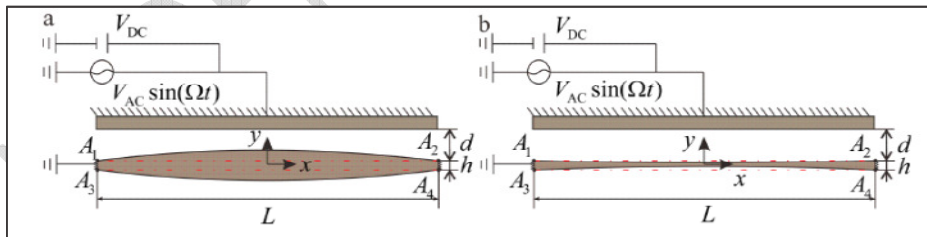
111 In this work, we have studied the reducing of the vibration system that is described in [24]
 112 through dynamic analysis by applying both of active control and time delay control. The effect of
 113 the varying parameters of the system and comparing between the two controllers have reported.

Comment [WU5]: This paragraph must show a summary of the work done by other researchers and the gap left by those researches which will also be your research interest.

115 **2. Equation of Motion**

116 Feng et al [24] have been studied a model considering the effect of surface machining error
 117 on the thickness of the microbeam. The thickness of the microbeam is not constant due to the
 118 processing errors. The schematic diagram of microbeam is shown in Fig. (1). The shape of the
 119 microbeam is controlled by adjusting the value of section parameter λ . (a) case of $\lambda > 0$ (b)
 120 case of $\lambda < 0$.

Comment [WU6]: What is processing error, you are not fabricating, then why thickness is not uniform in simulation environment explain with justifications.



122 **Fig. (1): The schematic diagram of microbeam.**

123 The bending vibration equation of the system is obtained through force analysis. Since the
 124 main objective of [24] was to explore the main resonance problem in the nonlinear dynamics
 125 problem, the first-order mode is considered that it was sufficient to obtain good results. So,
 126 Galerkin method is applied to derive a reduced-order model, they expressed the deflection $y(x,t)$

Comment [WU7]: Re-write and explain what you want to say in this line.

129 as: $y(x,t) = u(t)\phi(x)$, where $u(t)$ is the modal coordinate amplitude and $\phi(x)$ is the mode shapes
 130 of the normalized undamped linear orthonormal.

Comment [WU8]: Explain

131 The resonance frequency and bifurcation behavior can be obtained through dynamic analysis.
 132 Feng et al [24] introduced the modal coordinate amplitude through dynamic analysis using the
 133 MMS to investigate the response of the microresonator with small vibration amplitude around
 134 the stable equilibrium positions as $u = u_s + u_A$, where

135 u_s is the response to DC voltage and u_A is the response to AC voltage. The terms representing
 136 the equilibrium position can be eliminated in the equation of motion that governs the transverse
 137 deflection. Since V_{AC} is far less than V_{DC} in the microresonator, the terms
 138 $V_{DC} = O(1)$, $V_{AC} = O(\varepsilon^3)$ and ε is regarded as a small non-dimensional parameter. So, Feng et al
 139 [24] modified the equation of the system as follows:

$$140 \ddot{u}_A + \omega_n^2 u_A + \varepsilon^2 \mu \dot{u}_A + a_q u_A^2 + a_c u_A^3 = \varepsilon^3 f \cos(\omega t) \quad (1)$$

141 where:

142 u_A is the modal coordinate amplitude which to AC voltage, ω_n is the internal frequency, μ is the
 143 damping coefficient of the system, ω is the alternating current excitation frequency, f is the
 144 external excitation force, a_c and a_q are the nonlinear parameters.

Comment [WU9]: All these equations are seems to be taken from some source are not referenced, and not well explained.

145 3.1. Active Control

146 Using a negative linear velocity feedback controller connected to the nonlinear dynamical
 147 system; eqn. (1) can be represented as follows:

$$148 \ddot{u} + \omega^2 u + \varepsilon^2 \mu \dot{u} + a_q u^2 + a_c u^3 = \varepsilon^3 f \cos(\Omega t) - \varepsilon^2 G \dot{u} \quad (2)$$

149 We use the method of multiple scale

$$150 u(t, \varepsilon) = \varepsilon u_1(T_0, T_1, T_2) + \varepsilon^2 u_2(T_0, T_1, T_2) + \varepsilon^3 u_3(T_0, T_1, T_2) \quad (3)$$

151 where $T_k = \varepsilon^k t$. So, we can write that:

$$152 \frac{d}{dt} = D_0 + \varepsilon D_1 + \varepsilon^2 D_2 + \dots, \quad \frac{d^2}{dt^2} = D_0^2 + \varepsilon(2D_0 D_1) + \varepsilon^2(D_1^2 + 2D_0 D_2) + \dots \quad (4)$$

153 where $D_k = \frac{\partial}{\partial T_k}$, ($k=0,1,2$).

154 Substituting equations (3) and (4) into equations (2), then equating the like order of ε , we get
 155 the following:

156 Order ε^1 :

$$157 (D_0^2 + \omega^2) u_1 = 0 \quad (5)$$

158 Order ε^2 :

$$159 (D_0^2 + \omega^2) u_2 = -2D_0 D_1 u_1 - a_q u_1^2 \quad (6)$$

160 Order ε^3 :

$$161 (D_0^2 + \omega^2) u_3 = -2D_0 D_1 u_2 - (D_1^2 + 2D_0 D_2 + \mu D_0) u_1 - 2a_q u_1 u_2 - a_c u_1^3 + f \cos(\Omega t) - G D_0 u_1 \quad (7)$$

162 The general solution of equation (5) can be expressed in the form:

$$163 u_1 = A(T_1, T_2) e^{i\omega T_0} + \bar{A}(T_1, T_2) e^{-i\omega T_0} \quad (8)$$

164 Substituting equation (8) into equation (6), we can obtain the following:

Comment [WU10]: Why is this "So" important to use here and throughout this paper

$$165 \quad (D_0^2 + \omega^2)u_2 = -2i\omega \left[\left(\frac{\partial A}{\partial T_1} \right) e^{i\omega T_0} - \left(\frac{\partial \bar{A}}{\partial T_1} \right) e^{-i\omega T_0} \right] - a_q \left[A^2 e^{2i\omega T_0} + 2A\bar{A} + \bar{A}^2 e^{-2i\omega T_0} \right] \quad (9)$$

166 The secular term is eliminated if:

$$167 \quad -2i\omega \left(\frac{\partial A}{\partial T_1} \right) + cc. = 0 \quad \rightarrow \quad \left(\frac{\partial A}{\partial T_1} \right) = 0 \quad (10)$$

168 which indicates that A is only a function of T_2 .

169 We get one resonance case as the primary resonance case: $\Omega \cong \omega$

170 So, we can represent the detuning parameter σ as follows:

$$171 \quad \Omega = \omega + \varepsilon^2 \sigma \quad (11)$$

172 , the general solution of eqns. (6) and (7) can be written as:

$$173 \quad u_2 = \frac{a_q}{3\omega^2} A^2 e^{2i\omega T_0} - \frac{2a_q}{\omega^2} A\bar{A} + \frac{a_q}{3\omega^2} \bar{A}^2 e^{-2i\omega T_0} \quad (12)$$

$$174 \quad u_3 = \left(\frac{a_c}{8\omega^2} + \frac{1a_q^2}{12A\omega^4} \right) A^3 e^{3i\omega T_0} + cc. \quad (13)$$

175 By eliminating the secular term in eqn. (7), we get that:

$$176 \quad -2i\omega(D_2 A) - i\omega\mu A - 3a_c A^2 \bar{A} + \frac{10a_q^2}{3\omega^2} A^2 \bar{A} - i\omega G A + \frac{f}{2} e^{i\sigma T_2} = 0 \quad (14)$$

177 It is convenient to express A in the polar form:

$$178 \quad A = \frac{1}{2} a(T_2) e^{i\beta(T_2)} \quad (15)$$

179 By substituting eqn. (15) into eqn. (14); separating the imaginary and real parts yield:

$$180 \quad \dot{a} = - \left(\frac{\mu + G}{2} \right) a + \frac{f}{2\omega} \sin \theta \quad (16)$$

$$181 \quad a(\sigma - \dot{\theta}) = \left(\frac{3a_c}{8\omega} - \frac{5a_q^2}{12\omega^3} \right) a^3 - \frac{f}{2\omega} \cos \theta \quad (17)$$

$$182 \quad \text{Where, } \theta = \sigma T_2 - \beta \quad (18)$$

183 The steady-state response can be obtained by imposing the conditions: $\dot{a} = \dot{\theta} = 0$

184 By applying the previous conditions, the frequency response equation can be derived as follows:

$$185 \quad \sigma^2 - \left(\frac{3a_c}{4\omega} - \frac{5a_q^2}{6\omega^3} \right) a^2 \sigma + \left(\frac{3a_c}{8\omega} - \frac{5a_q^2}{12\omega^3} \right)^2 a^4 + \left(\frac{G + \mu}{2} \right)^2 - \left(\frac{f}{2\omega a} \right)^2 = 0 \quad (19)$$

186

187 3.1.1. Linear Solution

188 To study the stability of the linear solution of the obtained fixed points, let us consider A , in
189 the form:

$$190 \quad A(T_2) = \frac{1}{2} (p - iq) e^{i\gamma T_2} \quad (20)$$

191 By substituting from eqn. (20) into the linear parts of eqn. (14) and equating real and imaginary
192 parts; we get:

193 $\dot{p} = -\left(\frac{\mu+G}{2}\right)p - \gamma q$

194 (21)

195 $\dot{q} = \gamma p - \left(\frac{\mu+G}{2}\right)q$ (22)

196 The Characteristic equation can be written as:

197 $\left[\lambda + \left(\frac{\mu+G}{2}\right)\right]^2 + \gamma^2 = 0$ (23)

198 Easily we can deduce the solutions of the eqn. (23) as following:

199 $\lambda_{1,2} = -\left(\frac{\mu+G}{2}\right) \pm i\gamma$ (24)

200 So, the linear solution is stable everywhere that the real part is always negative.

201

202 3.1.2 Nonlinear solution:

203 To study the stability of the nonlinear solution of the obtained fixed points, let:

204 $a = a_0 + a_1, \theta = \theta_0 + \theta_1$ (25)

205 where a_0, θ_0 are the solutions of eqns. (16) and (17) and a_1, θ_1 are perturbations which are
206 assumed to be small compared with a_0, θ_0 .

207 Substituting equation (25) into equations (16) and (17) and keeping only the linear terms in a_1, θ_1
208 , gives:

209 $\dot{a}_1 = -\left(\frac{\mu+G}{2}\right)a_1 + \frac{f}{2\omega} \cos(\theta_0)\theta_1$ (26)

210 $\dot{\theta}_1 = \left(\frac{\sigma}{a_0} - \left(\frac{9a_c}{8\omega} - \frac{5a_q^2}{4\omega^3}\right)a_0\right)a_1 - \frac{f}{2\omega a_0} \sin(\theta_0)\theta_1$ (27)

211 We can express the characteristic equation as:

212 $\lambda^2 + \left(\frac{f}{2\omega a_0} \sin(\theta_0) + \left(\frac{\mu+G}{2}\right)\right)\lambda - \left(\frac{\sigma}{a_0} - \left(\frac{9a_c}{8\omega} - \frac{5a_q^2}{4\omega^3}\right)a_0\right)\frac{f}{2\omega} \cos(\theta_0)$
213 $+ \left(\frac{\mu+G}{2}\right)\frac{f}{2\omega a_0} \sin(\theta_0) = 0$ (28)

214 So, the solutions of eqn. (29) are:

215 $\lambda_{1,2} = -\frac{1}{4}\left(\mu+G + \frac{f}{\omega a_0} \sin(\theta_0)\right) \pm \frac{1}{4}\sqrt{\left(\mu+G + \frac{f}{\omega a_0} \sin(\theta_0)\right)^2 - 16K}$ (29)

216 where $K = \left(\frac{\mu+G}{2}\right)\frac{f}{2\omega a_0} \sin(\theta_0) - \left(\frac{\sigma}{a_0} - \left(\frac{9a_c}{8\omega} - \frac{5a_q^2}{4\omega^3}\right)a_0\right)\frac{f}{2\omega} \cos(\theta_0)$

217 (30)

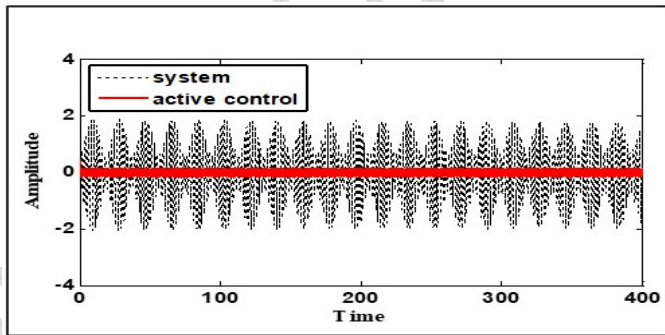
218 If the real part of the eigenvalue is negative, then the linear solution is stable; otherwise, it is
219 unstable.

220

221
222
223
224
225
226
227
228
229
230
231
232
233
234
235
236
237
238
239
240
241

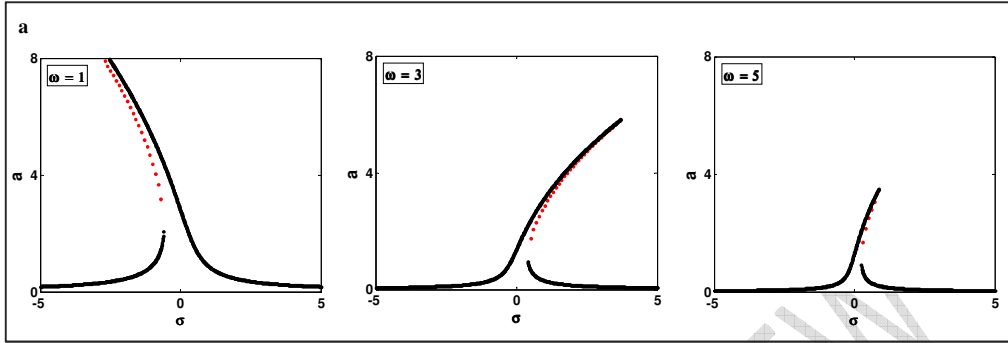
3.1.3. Numerical Solution

The Runge-Kutta fourth-order method has been applied to determine the numerical solution of the equation (2) as shown in Figure 2 at the selected values: ($\Omega = 3.066$, $\omega = 3.066$, $\mu = 0.003$, $a_q = 1, a_c = 1, f = 1.8, G = 4$). Figure 2 shows the effect of using active control on the amplitude of the main system. Numerical solution of the response equation represented in equation (19) have been discussed. Figure 3 illustrates the effect of the varying parameters on the response curve at the primary resonance case $\Omega \cong \omega$ under effect of the gain feedback controller. The solid line represents the stable region. While, the dotted line represents the unstable region. Figure (3a) shows that the parameter of the natural frequency has hardening and softening nonlinearity effect. The effect of the damping coefficient on the response curve is illustrated in Figure (3b). It shows that the amplitude is monotonic decreasing function and the amplitude is bent to right. The effect of nonlinear parameters is shown in Figures (3c) and (3d). Figure (3c) shows that the amplitude is monotonic decreasing function in the nonlinear parameter a_c and the amplitude is bent to right. Figure (3d) shows that the nonlinear parameter a_q has hardening and softening nonlinearity effect. The amplitude is monotonic increasing with varying of the excitation force f and the amplitude is bent to right. It is shown in Figure (3e). Figure (3f) illustrates that the amplitude is monotonic decreasing function in the parameter of gain feedback controller G .



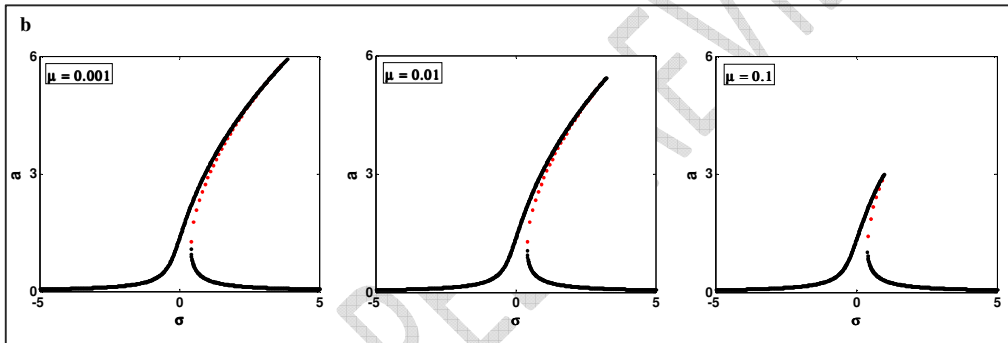
242
243
244
245

Fig. (2): The time history of the main system and active control at primary resonance case $\Omega \cong \omega$



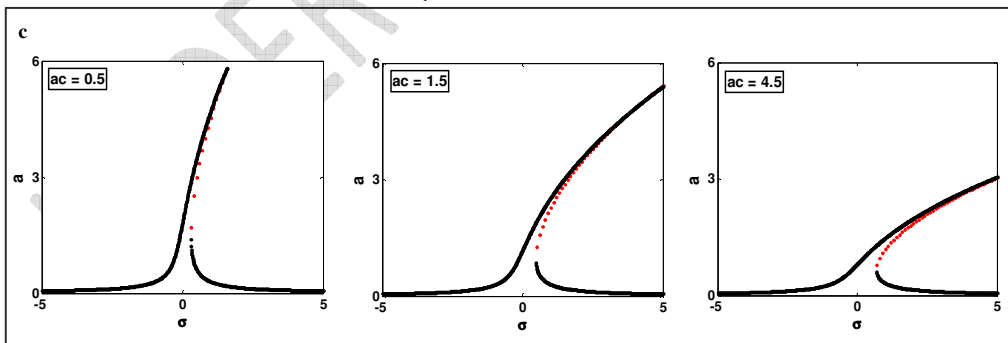
246
247 **Fig. (3a): effect of ω , the values of the parameters are: $\mu = 0.003, a_q = 1, a_c = 1, f = 1.8, G = 0.1$**

248
249



250
251 **Fig. (3b): effect of μ , the values of the parameters are:**
252 $\omega = 3.066, a_q = 1, a_c = 1, f = 1.8, G = 0.1.$

250
251
252



253
254 **Fig. (3c): effect of a_c , the values of the parameters are:**
255 $\omega = 3.066, \mu = 0.003, a_q = 1, f = 1.8, G = 0.1.$

253
254
255
256

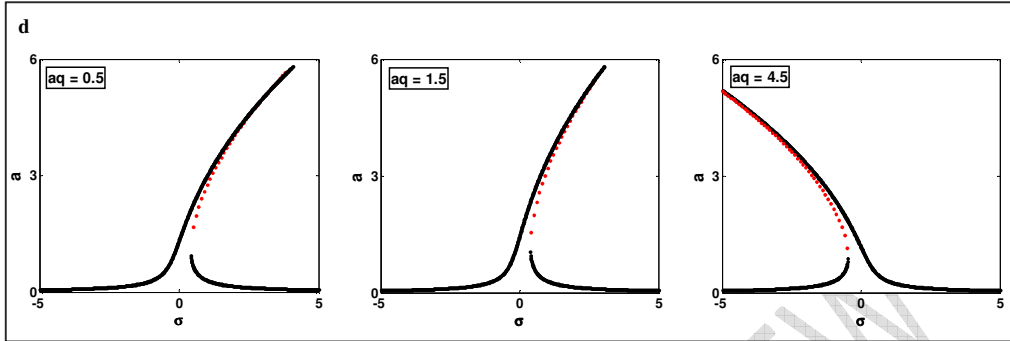


Fig. (3d): effect of a_q , the values of the parameters are:

$$\omega = 3.066, \mu = 0.003, a_c = 1, f = 1.8, G = 0.1.$$

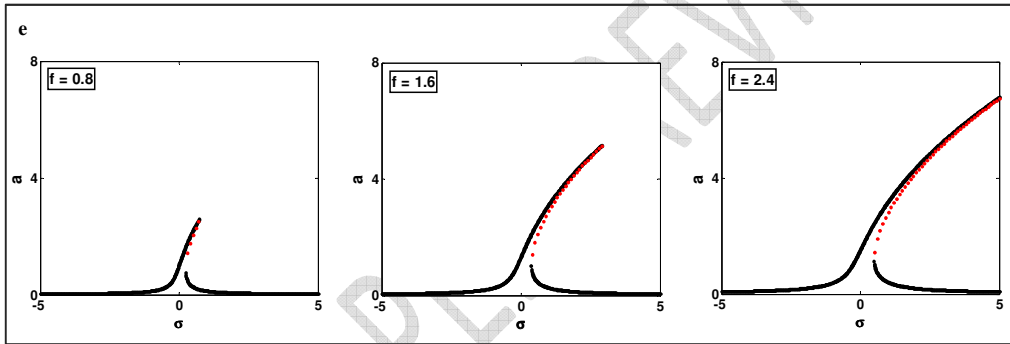


Fig. (3e): effect of f , the values of the parameters are:

$$\omega = 3.066, \mu = 0.003, a_c = 1, a_q = 1, G = 0.1.$$

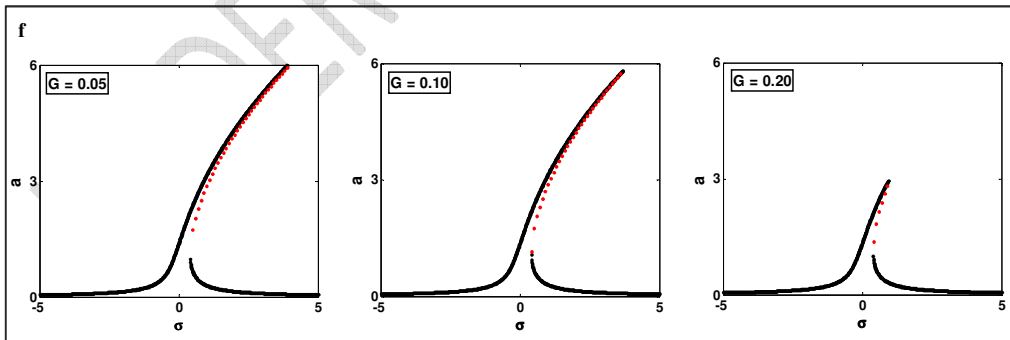


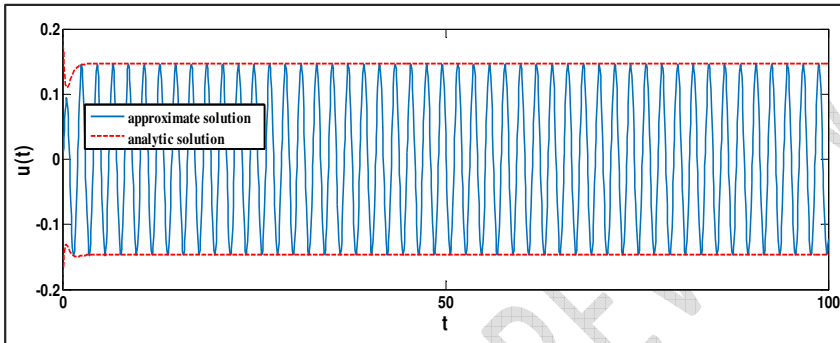
Fig. (3f): effect of G , the values of the parameters are:

$$\omega = 3.066, \mu = 0.003, a_c = 1, a_q = 1, f = 1.8.$$

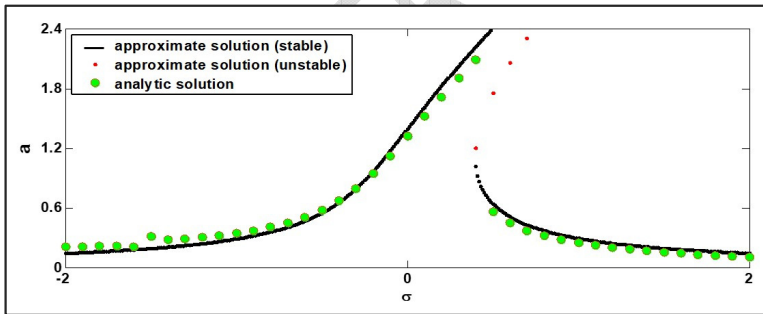
270 **3.1.4. Comparison between the perturbation and the numerical solution**

271 The comparison of the analytical solution - given by equations (26) and (27) - and the
 272 approximate solution of equation (2) at the case of active control have been shown in Figure (4)
 273 and Figure (5). Figure (4) described the comparison in the time history and Figure (5) described
 274 the comparison in the response curve. Figures (4) and (5) show that there is a good agreement
 275 between both analytical and numerical solutions.
 276

Comment [WU11]: Explain the findings from this analyses in detail



277 **Fig. (4): Comparison between the analytic solution and the approximate solution at the case**
 278 **of active control (Time history).**
 279
 280



281 **Fig. (5): Comparison between the analytic solution and the approximate solution at the case**
 282 **of active control (Response curve).**
 283
 284

285 **3.2. Time delay Control:**

286 The equation of system under consideration using time delay control is represented as
 287 follows:

$$288 \ddot{u}(t) + \omega^2 u(t) + \varepsilon^2 \mu \dot{u}(t) + a_q u^2(t) + a_c u^3(t) = \varepsilon^3 f \cos(\Omega t) - \varepsilon^2 G \dot{u}(t - \tau) \quad (31)$$

289 The secular term will be:

$$290 -2i\omega(D_2 A) - i\omega\mu A - 3a_c A^2 \bar{A} + \frac{10a_q^2}{3\omega^2} A^2 \bar{A} - i\omega G A e^{-i\omega\tau} + \frac{f}{2} e^{i\sigma T_2} = 0 \quad (32)$$

291 By substituting eqn. (15) into eqn. (32); separating the imaginary and real parts yield:

$$292 \dot{a} = -\frac{\mu}{2} a - \frac{G}{2} a \cos(\omega\tau) + \frac{f}{2\omega} \sin \theta \quad (33)$$

Comment [WU12]: What will be the benefits of Time delay and its control please explain.

$$293 \quad a(\sigma - \dot{\theta}) = \frac{G}{2} a \sin(\omega\tau) + \left(\frac{3a_c}{8\omega} - \frac{5a_q^2}{12\omega^3} \right) a^3 - \frac{f}{2\omega} \cos\theta \quad (34)$$

294 Finally, by applying the conditions $\dot{a} = \dot{\theta} = 0$; the frequency response equation can be derived as
295 follows:

$$296 \quad \sigma^2 - \left[\left(\frac{3a_c}{4\omega} - \frac{5a_q^2}{6\omega^3} \right) a^2 + G \sin(\omega\tau) \right] \sigma + \left(\frac{3a_c}{8\omega} - \frac{5a_q^2}{12\omega^3} \right)^2 a^4 + \left(\frac{3a_c}{8\omega} - \frac{5a_q^2}{12\omega^3} \right) Ga^2 \sin(\omega\tau) + \frac{\mu G}{2} \cos(\omega\tau) \\ 297 \quad + \frac{\mu^2 + G^2}{4} - \left(\frac{f}{2\omega a} \right)^2 = 0 \quad (35)$$

298 3.2.1. Linear Solution

299 Put: $A(T_2) = \frac{1}{2}(p - iq)e^{i\gamma T_2}$ into the linear parts of eqn. (32) to study the stability of the linear
300 solution; we get after equating real and imaginary parts:

$$301 \quad \dot{p} = - \left(\frac{\mu}{2} + \frac{G}{2} \cos(\omega\tau) \right) p - \left(\gamma - \frac{G}{2} \sin(\omega\tau) \right) q \quad (36)$$

$$302 \quad \dot{q} = \left(\gamma - \frac{G}{2} \sin(\omega\tau) \right) p - \left(\frac{\mu}{2} + \frac{G}{2} \cos(\omega\tau) \right) q \quad (37)$$

303 The Characteristic Eqn. can be expressed as follows:

$$304 \quad 4\lambda^2 + 4(\mu + G \cos(\omega\tau))\lambda + (\mu^2 + G^2 + 4\gamma^2 + 2\mu G \cos(\omega\tau) - 4\gamma G \sin(\omega\tau)) = 0 \quad (38)$$

305 The solutions of eqn. (38) are:

$$306 \quad \lambda_{1,2} = \frac{1}{2}(\mu + G \cos(\omega\tau)) \pm \frac{1}{2} \sqrt{(\mu + G \cos(\omega\tau))^2 - (\mu^2 + G^2 + 4\gamma^2 + 2\mu G \cos(\omega\tau) - 4\gamma G \sin(\omega\tau))} \quad (39)$$

307 So; the linear solution is stable only if the real part of the eigenvalue in eqn. (39) is negative.

308

309 3.2.2. Nonlinear Solution

310 Putting: $a = a_0 + a_1$, $\theta = \theta_0 + \theta_1$ into eqns. (33) and (34); we can deduce that:

$$311 \quad \dot{a}_1 = - \left(\frac{\mu}{2} + \frac{G}{2} \cos(\omega\tau) \right) a_1 + \frac{f}{2\omega} \cos(\theta_0) \theta_1 \quad (40)$$

$$312 \quad \dot{\theta}_1 = \left(\frac{\sigma}{a_0} - \frac{G}{2a_0} \sin(\omega\tau) - \left(\frac{9a_c}{8\omega} - \frac{5a_q^2}{4\omega^3} \right) a_0 \right) a_1 - \frac{f}{2\omega a_0} \sin(\theta_0) \theta_1 \quad (41)$$

313 We can write the characteristic equation and its solutions as follows:

$$314 \quad \lambda^2 + \frac{1}{2} \left(\mu + G \cos(\omega\tau) + \frac{f}{\omega a_0} \sin(\theta_0) \right) \lambda + H = 0$$

315 (42)

$$316 \quad \text{where } H = \left(\frac{\mu}{2} + \frac{G}{2} \cos(\omega\tau) \right) \frac{f}{2\omega a_0} \sin(\theta_0) - \left(\frac{\sigma}{a_0} - \frac{G}{2a_0} \sin(\omega\tau) - \left(\frac{9a_c}{8\omega} - \frac{5a_q^2}{4\omega^3} \right) a_0 \right) \frac{f}{2\omega} \cos(\theta_0)$$

$$\lambda_{1,2} = \frac{1}{4} \left(\mu + G \cos(\omega\tau) + \frac{f}{\omega a_0} \sin(\theta_0) \right) \pm \frac{1}{8} \sqrt{\left(\mu + G \cos(\omega\tau) + \frac{f}{\omega a_0} \sin(\theta_0) \right)^2 + 64H} \quad (43)$$

318 If the real part of the eigenvalue is negative, then the linear solution is stable; otherwise, it is
 319 unstable.

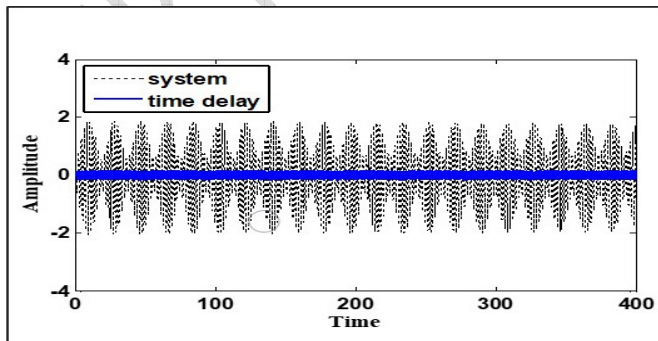
320

3.2.3. Numerical Solution:

322 The Runge-Kutta fourth-order method has been applied to determine the numerical solution
 323 of the equation (31) as shown in Figure 6 at the selected values:
 324 ($\Omega = 3.066$, $\omega = 3.066$, $\mu = 0.003$,

325 $a_q = 1$, $a_c = 1$, $f = 1.8$, $G = 4$, $\tau = 0.1$). Figure 6 shows the effect of using time delay control on the
 326 amplitude of the main system. Numerical solution of the response equation represented in
 327 equation (35) have been discussed. Figure 7 illustrates the effect of the varying parameters on the
 328 response curve at the primary resonance case $\Omega \cong \omega$ under effect of the time delay controller.
 329 The solid line represents the stable region. While, the dotted line represents the unstable region.
 330 Figure (7a) shows that the parameter of the natural frequency has hardening and softening
 331 nonlinearity effect. The effect of the damping coefficient on the response curve is illustrated in
 332 Figure (7b). It shows that the amplitude is monotonic decreasing function and the amplitude is
 333 bent to right. The effect of nonlinear parameters is shown in Figures (7c) and (7d). Figure (7c)
 334 shows that the amplitude is monotonic decreasing function in the nonlinear parameter a_c and the
 335 amplitude is bent to right. Figure (7d) shows that the nonlinear parameter a_q has hardening and
 336 softening nonlinearity effect. The amplitude is monotonic increasing with varying of the
 337 excitation force f and the amplitude is bent to right. It is shown in Figure (7e). Figure (7f)
 338 illustrates that the amplitude is monotonic decreasing function in the parameter of gain feedback
 339 controller G . Fig. (7g) shows that the amplitude is monotonic increasing function in the
 340 parameter of time delay controller τ .

341



342

343

344

Fig. (6): The time history of the main system and time delay control at primary resonance case $\Omega \cong \omega$

345

3.2.4. Comparison between the perturbation and the numerical solution

346

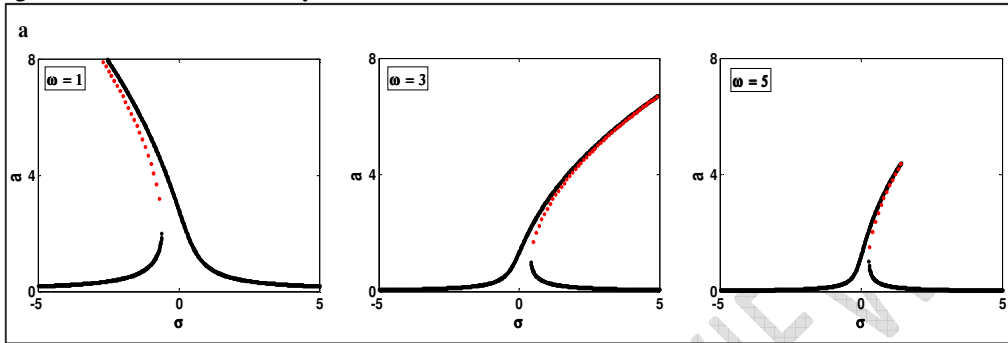
347

348

The comparison of the analytical solution - given by equations (40), (41) and the approximate solution of equation (31) at the case of time delay control have been shown in Figure (8) and Figure (9). Figure (8) described the comparison in the time history and Figure (9)

Comment [WU13]: Please highlight the findings of comparisons in bullets. Good agreement between both analytical and numerical solutions does not satisfy the reader.

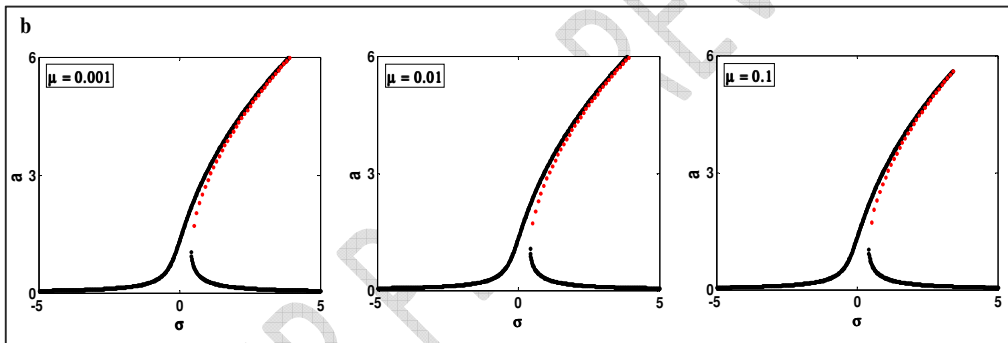
349 described the comparison in the response curve. Figures (8) and (9) show that there is a good
350 agreement between both analytical and numerical solutions.



351 **Fig. (7a): effect of ω , the values of the parameters are:**

352 $\mu = 0.003, a_q = 1, a_c = 1, f = 1.8, G = 0.1, \tau = 0.1.$

353
354



355 **Fig. (7b): effect of μ , the values of the parameters are:**

356 $\omega = 3.066, a_q = 1, a_c = 1, f = 1.8, G = 0.1, \tau = 0.1.$

357
358
359

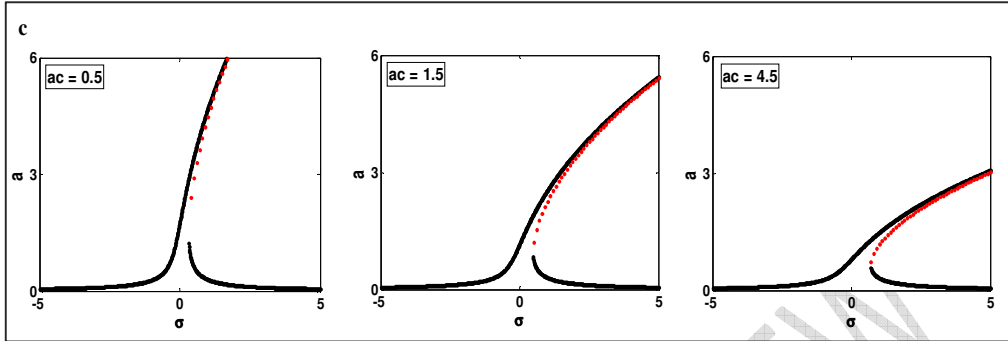


Fig. (7c): effect of a_c , the values of the parameters are:

$$\omega = 3.066, \mu = 0.003, a_q = 1, f = 1.8, G = 0.1, \tau = 0.1.$$

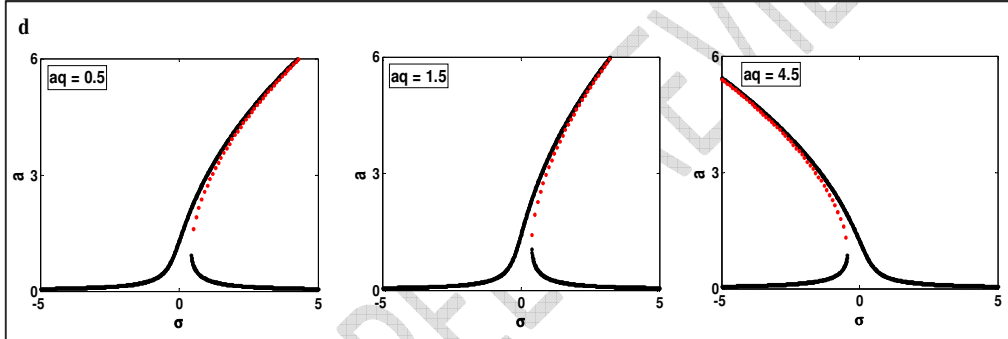


Fig. (7d): effect of a_q , the values of the parameters are:

$$\omega = 3.066, \mu = 0.003, a_c = 1, f = 1.8, G = 0.1, \tau = 0.1.$$

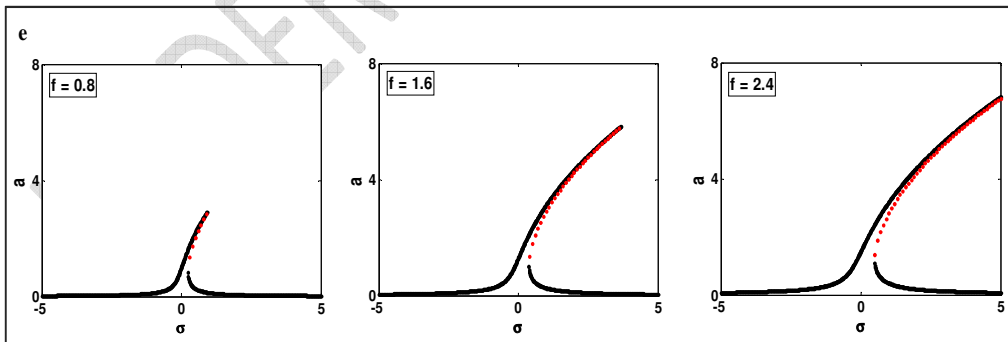
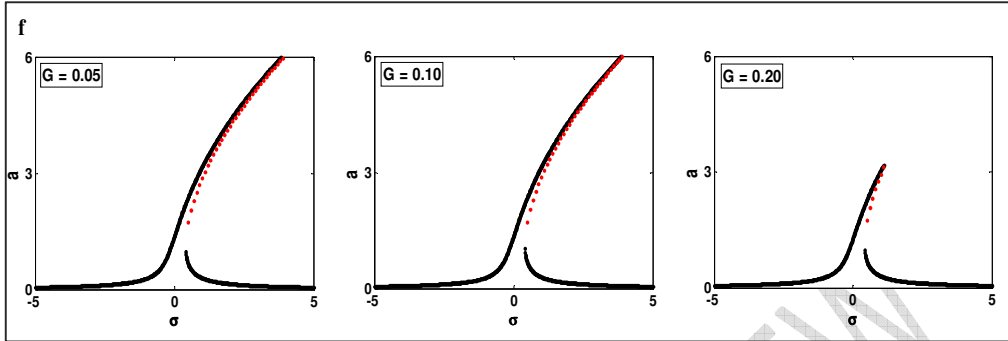


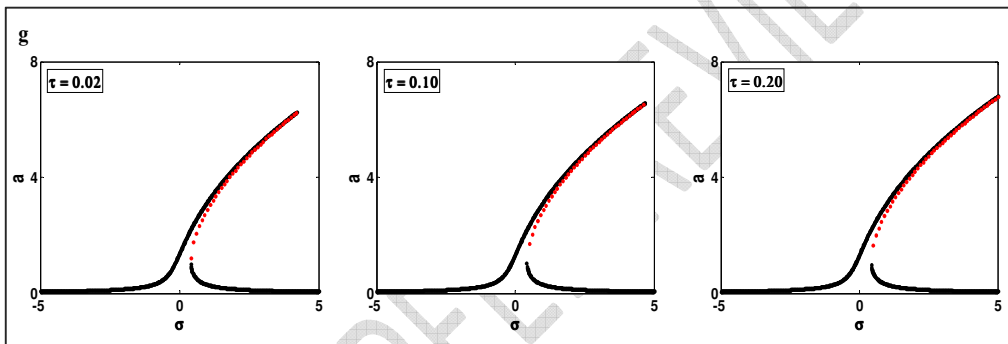
Fig. (7e): effect of f , the values of the parameters are:

$$\omega = 3.066, \mu = 0.003, a_c = 1, a_q = 1, G = 0.1, \tau = 0.1.$$



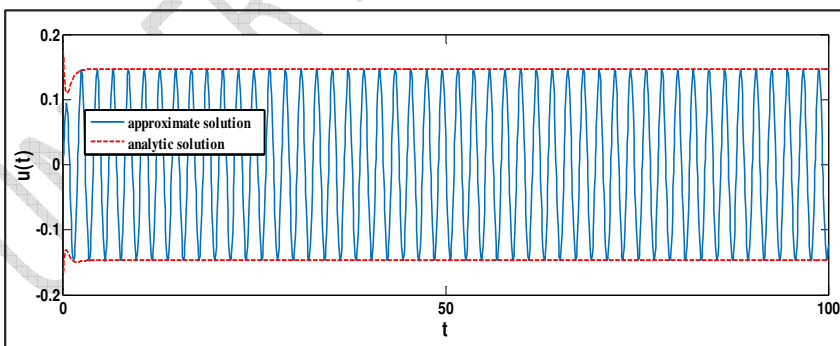
371
372
373

Fig. (7f): effect of G , the values of the parameters are:
 $\omega = 3.066, \mu = 0.003, a_c = 1, a_q = 1, f = 1.8, \tau = 0.1$.



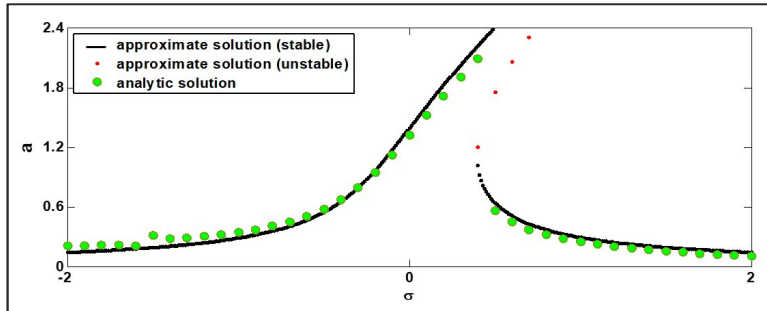
374
375
376
377

Fig. (7g): effect of τ , the values of the parameters are:
 $\omega = 3.066, \mu = 0.003, a_c = 1, a_q = 1, f = 1.8, G = 0.1$.



378
379
380
381

Fig. (8): Comparison between the analytic solution and the approximate solution at the case of time delay (Time history).



382
383 **Fig. (9): Comparison between the analytic solution and the approximate solution at the case**
384 **of time delay (Response curve).**

385 **4. Conclusion**

386 The resulted vibration of a nonlinear dynamic mechanical system of electrostatic MEMS
387 resonator subjected to external force has been studied to be controlled. Active control method is
388 applied to reduce this vibration via negative linear velocity feedback. Also, time delay controller
389 is used in reduction of the system vibration. The system is described by a unique differential
390 equation. Multiple Scale Perturbation Technique (MSPT) is applied to determine an approximate
391 solution for this system. The stability of the system near the primary resonance case is studied by
392 applying the frequency response equation. A numerical integration of the system behavior
393 without and with two controllers is studied. The results of this paper are reported:

- 394 1) Using negative gain feedback controller or time delay controller is effective in reduction
395 about 93% of the system vibration amplitude.
396 2) The effect of the negative gain feedback controller and the time delay controller is similar
397 in reduction of the system vibration amplitude.
398 3) The effectiveness of the controllers is about $E_a(u) = 2000$.

399 **References**

- 400 [1] B.Vazquez-Gonzalez and G.Silva-Navarro, Evaluation of the autoparametric pendulum
401 vibration absorber for a Duffing system, Shock and Vibration, 15 (2008) 355-368.
402 [2] M. Eissa, M. Kamel and A. T. El-Sayed, Vibration reduction of a nonlinear spring
403 pendulum under multi external and parametric excitations via a longitudinal absorber,
404 Meccanica, 46 (2011) 325-340.
405 [3] M. Sayed and M. Kamel, 1:2 and 1:3 internal resonance active absorber for non-linear
406 vibrating system, Applied Mathematical Modelling, 36 (2012) 310-332.
407 [4] D. Sado, The dynamics of a coupled three degree of freedom mechanical system,
408 Mechanics and Mechanical Engineering, 7 (2004) 29-40.
409 [5] G. Wenzhi and H. Zhiyong, Active control and simulation test study on torsional
410 vibration of large turbo-generator rotor shaft, Mechanism and Machine Theory, 45 (2010)
411 1326-1336.
412 [6] Y. A. Amer, H. S. Bauomy and M. Sayed, Vibration suppression in a twin-tail system to
413 parametric and external excitation. Comput. Math. Appl., 58 (2009) 1947-1964.
414 [7] U. H. Hegazy and N. A. Salem, Nonlinear saturation controller for suppressing inclined
415 beam vibrations, International Journal of Scientific & Engineering Research, 7 (2016)
416 964-974.

Comment [WU14]: Where are these findings explained in the text.

- 417 [8] H. A. El-Gohary, W. A. A. El-Ganaini, Vibration suppression of a dynamical system to
418 multi-parametric excitations via time delay absorber, *Applied Mathematical Modelling*,
419 36 (2012) 35-45.
- 420 [9] A. Maccari, Arbitrary amplitude periodic solutions for parametrically excited systems
421 with time delay, *Nonlinear Dynamics*, 51 (2008) 111-126.
- 422 [10] A. M. Elnaggar and K. M. Khalil, The response of nonlinear controlled system under an
423 external excitation via time delay state feedback, *Journal of King Saud University –*
424 *Engineering Sciences*, 28 (2016) 75-83.
- 425 [11] A. F. El-Bassiouny and S. El-Kholy, Resonances of a nonlinear single-degree of freedom
426 system with time delay in linear feedback control, *Z. Naturforsch.* 65a (2010) 357-368.
- 427 [12] Y. S. Hamed and Y. A. Amer, Nonlinear saturation controller for vibration suppression of
428 a nonlinear flexible composite beam, *J. Mech. Sci. Technol.*, 2 (2014) 2987-3002.
- 429 [13] M. Kamel, A. Kandil, W. A. El-Ganaini and M. Eissa, Active vibration control of a
430 nonlinear magnetic levitation system via Nonlinear Saturation Controller (NSC),
431 *Nonlinear Dynamics*, 77 (2014) 605-619.
- 432 [14] J. Warminski, M. P. Cartmell, A. Mitura and M. Bochenski, Active vibration control of a
433 nonlinear beam with self and external excitations, *Shock and Vibration*, 20 (2013) 1033-
434 1047.
- 435 [15] Y. A. Amer, Vibration control of ultrasonic cutting via dynamic absorber, *Chaos,*
436 *Solutions & Fractals*, 33 (2007) 1703-1710.
- 437 [16] S. Ebrahimi, E. Salahshoor and M. Maasoomi, Application of the method of multiple
438 scales for nonlinear vibration analysis of mechanical systems with dry and lubricated
439 clearance joints, *Journal of Theoretical and Applied Vibration and Acoustics*, 3 (2017)
440 41-60.
- 441 [17] Y. A. Amer and M. N. Abd Elsalam, Stability and control of dynamical system subjected
442 to multi external forces, *International Journal of Mathematics and Computer*, 3 (2013)
443 41-52.
- 444 [18] S. Shahlaei-Far, A. Nabarrete, J. M. Balthazar, Homotopy analysis of a forced nonlinear
445 beam model with quadratic and cubic nonlinearities, *Journal of Theoretical and Applied*
446 *Mechanics*, 54 (2016) 1219-1230.
- 447 [19] D. Wang, Z. Hao, Y. Chen and Y. Zhang, Dynamic and resonance response analysis for a
448 turbine blade with varying rotating speed, *Journal of Theoretical and Applied Mechanics*,
449 56 (2018) 31-42.
- 450 [20] Y. S. Hamed, A. T. EL-Sayed and E. R. El-Zahar, On controlling the vibrations and
451 energy transfer in MEMS gyroscope system with simultaneous resonance, *Nonlinear*
452 *Dynamics*, 83 (2016) 1687-1704.
- 453 [21] A. Staino and B. Basu, Dynamics and control of vibrations in wind turbines with variable
454 rotor speed, *Engineering Structures*, 56 (2013) 58-67.
- 455 [22] S. Shaó, K.M. Masri and M.I. Younis, The effect of time-delayed feedback controller on
456 an electrically actuated resonator, *Nonlinear Dynamics*, 74 (2013) 257-270.
- 457 [23] M. Daqaq, C. Reddy and A. Nayfeh, Input-shaping control of nonlinear MEMS,
458 *Nonlinear Dynamics*, 54 (2008) 167-179.
- 459 [24] J. Feng, C. Liu, W. Zhang and S. Hao, Static and dynamic mechanical behaviors of
460 electrostatic MEMS resonator with surface processing error, *Micromachines*, 9 (2018)
461 34.